Supplementary Information

Low loading of Pt in radiation-synthesized Pt-MoS_x/KB nanocomposites for enhancing electrocatalytic hydrogen evolution reaction

Yicheng Wang,[a] Shuangxiao Li,[a] Xueyan Que,[c] Zeyu Zhang,[a] Ling Xu,[d] Yue Wang,[a] Jing Peng,[a] Jiuqiang Li,[a] Shuanglin Hu,[b] Yinyong Ao[b*] and Maolin Zhai[a*]

a. Beijing National Laboratory for Molecular Sciences, Radiochemistry and Radiation Chemistry Key Laboratory of Fundamental Science, The Key Laboratory of Polymer Chemistry and Physics of the Ministry of Education, College of Chemistry and Molecular Engineering, Peking University, Beijing 100871, China

b. Institute of Nuclear Physics and Chemistry, China Academy of Engineering Physics, Mianyang 621900, China

c. Yangling Hesheng Irradiation Technologies Co., Ltd., Yangling 712100, China

d. State Key Laboratory of Molecular Vaccinology and Molecular Diagnostics, School of Public Health, Xiamen University, Xiamen 161102, China

* Correspondence author:

Email address: aoyinyong@126.com (Y. Ao); mlzhai@pku.edu.cn (M. Zhai)

Table S1 Sample abbreviations, preparation conditions and corresponding loading of the as-prepared MoS_x/KBs (Ketjen Black as substrate, dose rate = 80 Gy/min).

Sample	Absorbed dose (kGy)	Ketjen black substrate (mg)	$(NH_4)_2MoS_4$ (mmol/L)	Loading of MoS_x (%)
MoS_x/KB-I	50	200	12.5	48.0
MoS_x/KB-II	100	200	12.5	48.3
MoS_x/KB-III	150	200	12.5	48.9
MoS_x/KB-IV	200	200	12.5	48.6
MoS_x/KB-V	250	200	12.5	49.1
MoS_x/KB-VI	300	200	12.5	47.9
MoS_x/KB-VII	100	200	0.66	3.2
MoS_x/KB-VIII	100	200	1.38	9.1
MoS_x/KB-IX	100	200	3.12	19.2
MoS_x/KB-X	100	200	5.36	29.0
MoS_x/KB-XI	100	200	8.34	37.9
MoS_x/KB-XII	100	200	12.5	48.3

Table S2 Sample abbreviations, preparation conditions and corresponding loading of the as-prepared Pt-MoS_x/KBs (MoS_x/KB-IX as substrate, dose rate = 25 Gy/min).

Sample	Absorbed dose (kGy)	MoS_x/KB-IX substrate (mg)	H_2PtCl_6 (mmol/L)	Loading of Pt (%)
Pt-MoS_x/KB-I	25	200	1.0	1.3
Pt-MoS_x/KB-II	25	200	2.1	3.3
Pt-MoS_x/KB-III	25	200	3.9	5.7
Pt-MoS_x/KB-IV	25	200	6.3	8.9
Pt-MoS_x/KB-V	25	200	9.8	13.9
Pt-MoS_x/KB-VI	5	200	9.8	11.9
Pt-MoS_x/KB-VII	10	200	9.8	12.3
Pt-MoS_x/KB-VIII	50	200	9.8	14.6
Pt-MoS_x/KB-IX	75	200	9.8	14.5

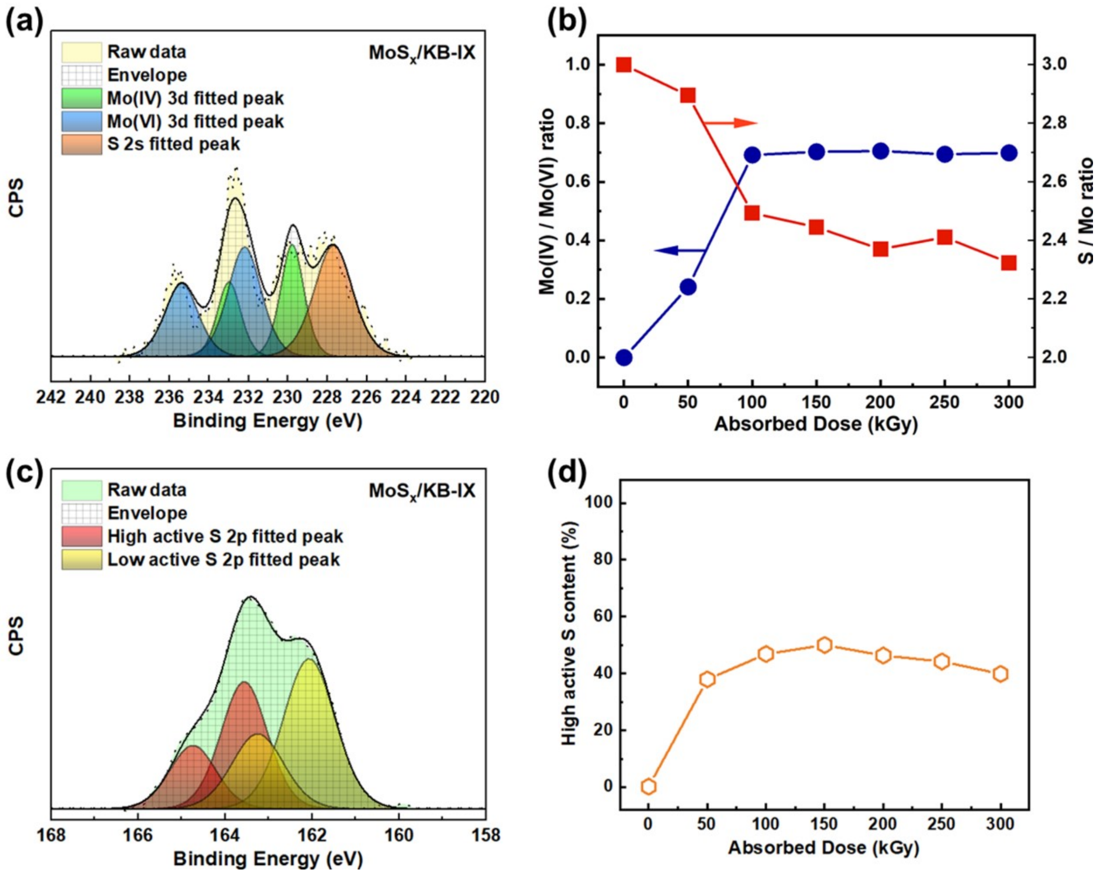

Fig. S1 (a) The deconvoluted Mo 3d high-resolution X-ray photoelectron spectrum of MoS_x/KB-IX; (b) The relationship curve of the Mo(IV)/Mo(VI) ratio and S/Mo ratio of MoS_x/KB catalysts with absorbed dose; (c) The deconvoluted S 2p high-resolution X-ray photoelectron spectrum of MoS_x/KB-IX; (d) The relationship curve of the high active S content of MoS_x/KB catalysts with absorbed dose.

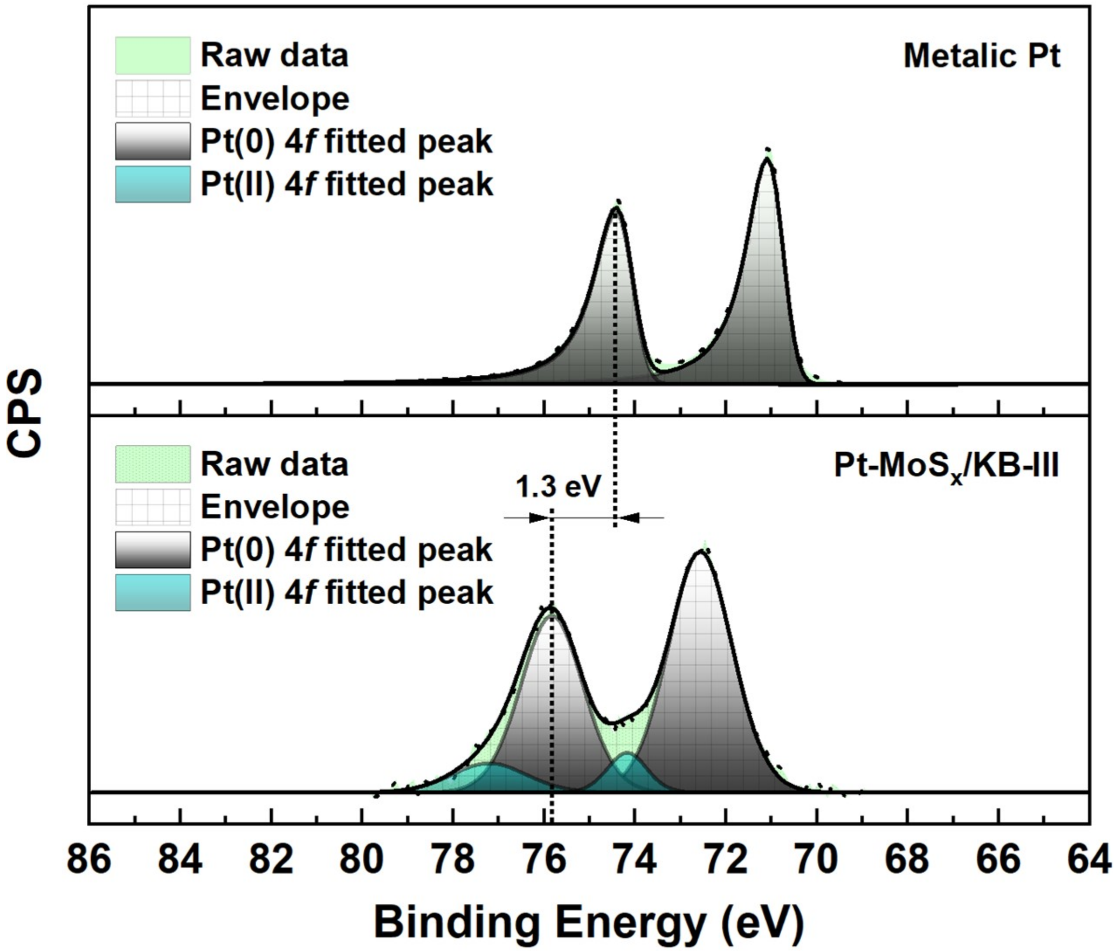

Fig. S2 Comparison of deconvoluted Pt 4f high-resolution XPS spectra of metallic Pt and Pt-MoS_x/KB-III.

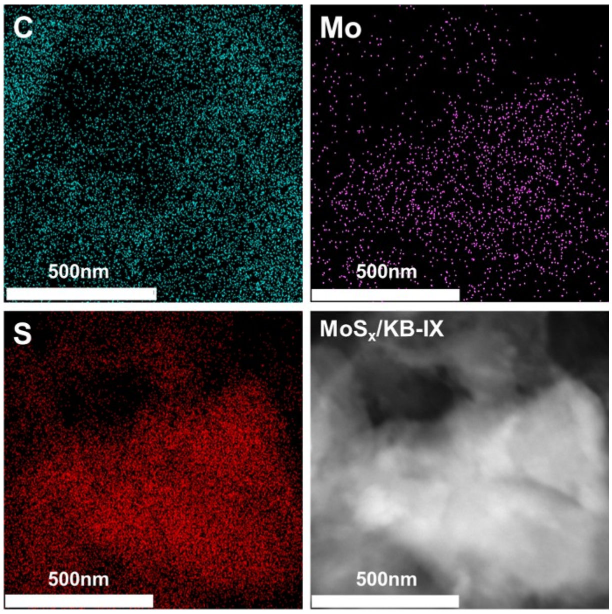

Fig. S3 the STEM-EDS mapping image of MoS_x/KB-IX.

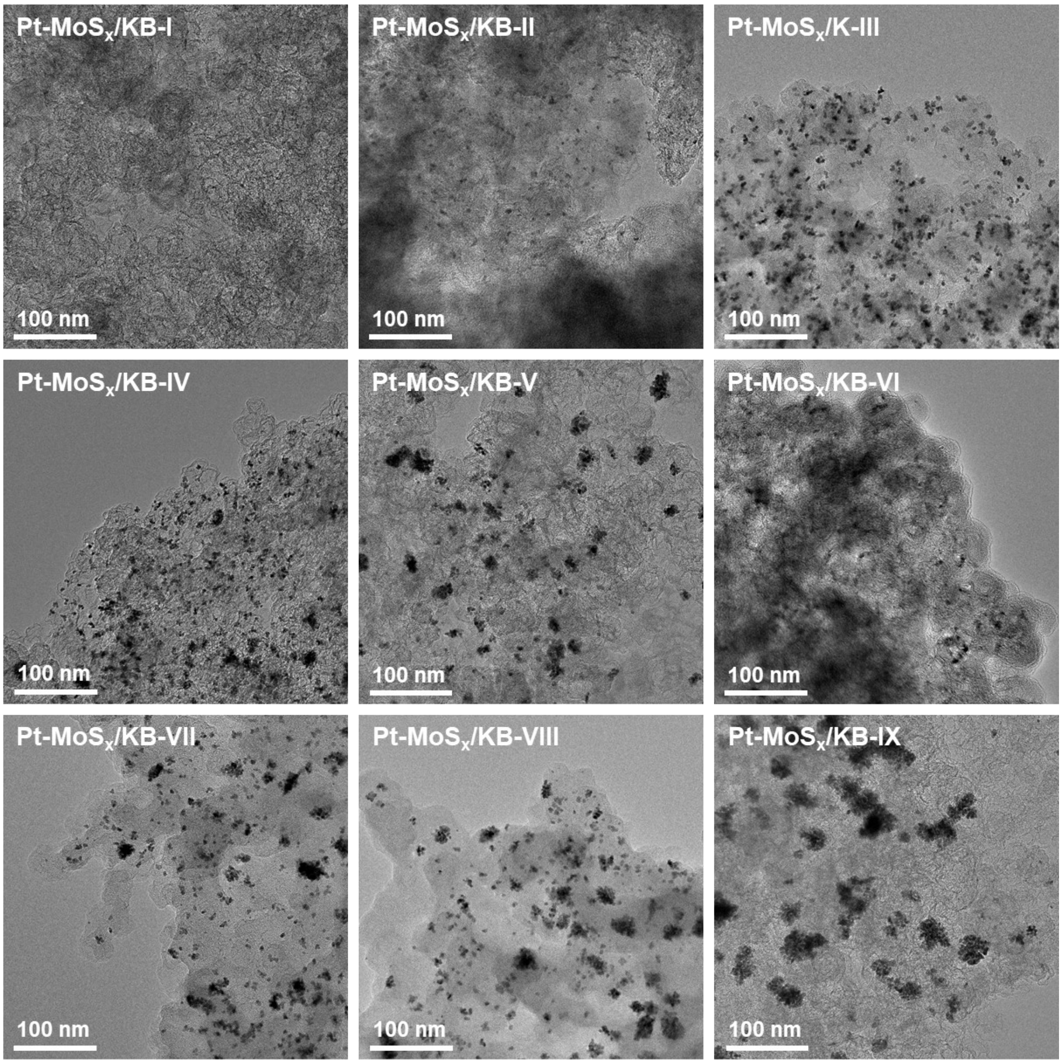

Fig. S4 The TEM image comparison of the as-synthesized Pt-MoS_x/KBs.

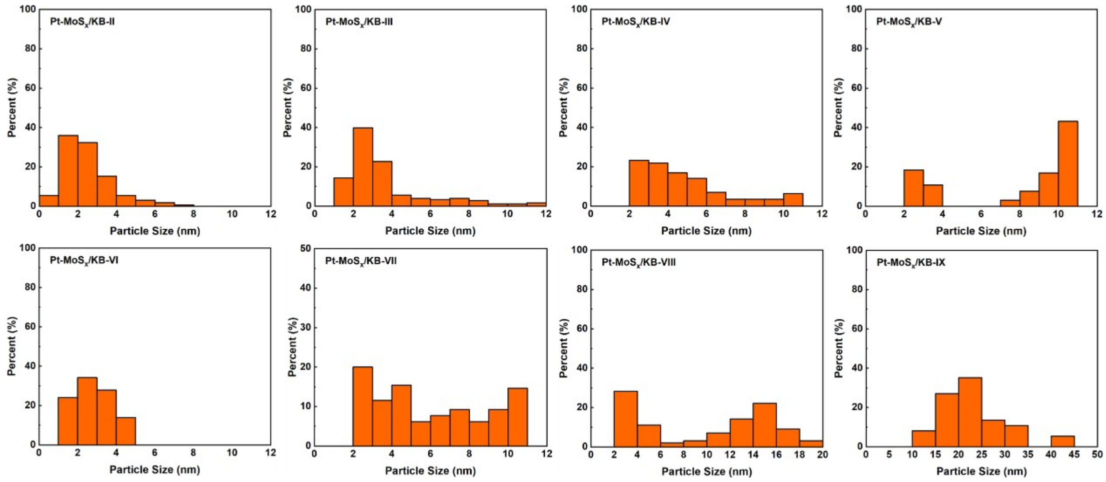

Fig. S5 The particle size distribution of Pt NPs in the as-synthesized Pt-MoS_x/KBs, which is calculated from their corresponding TEM images.

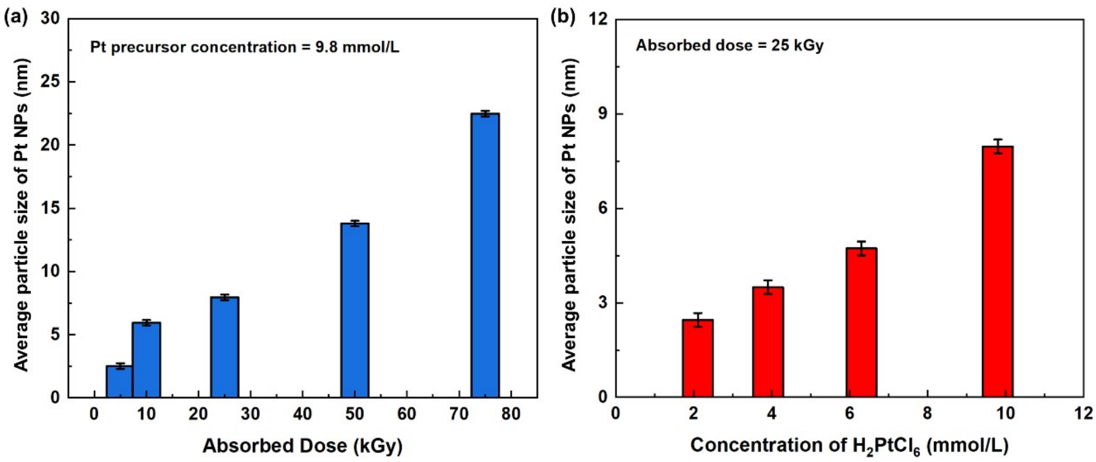

Fig. S6 The average-particle size of Pt NPs in the as-synthesized Pt-MoS_x/KBs under different absorbed doses (a) and different concentrations of H_2PtCl_6 precursor (b).

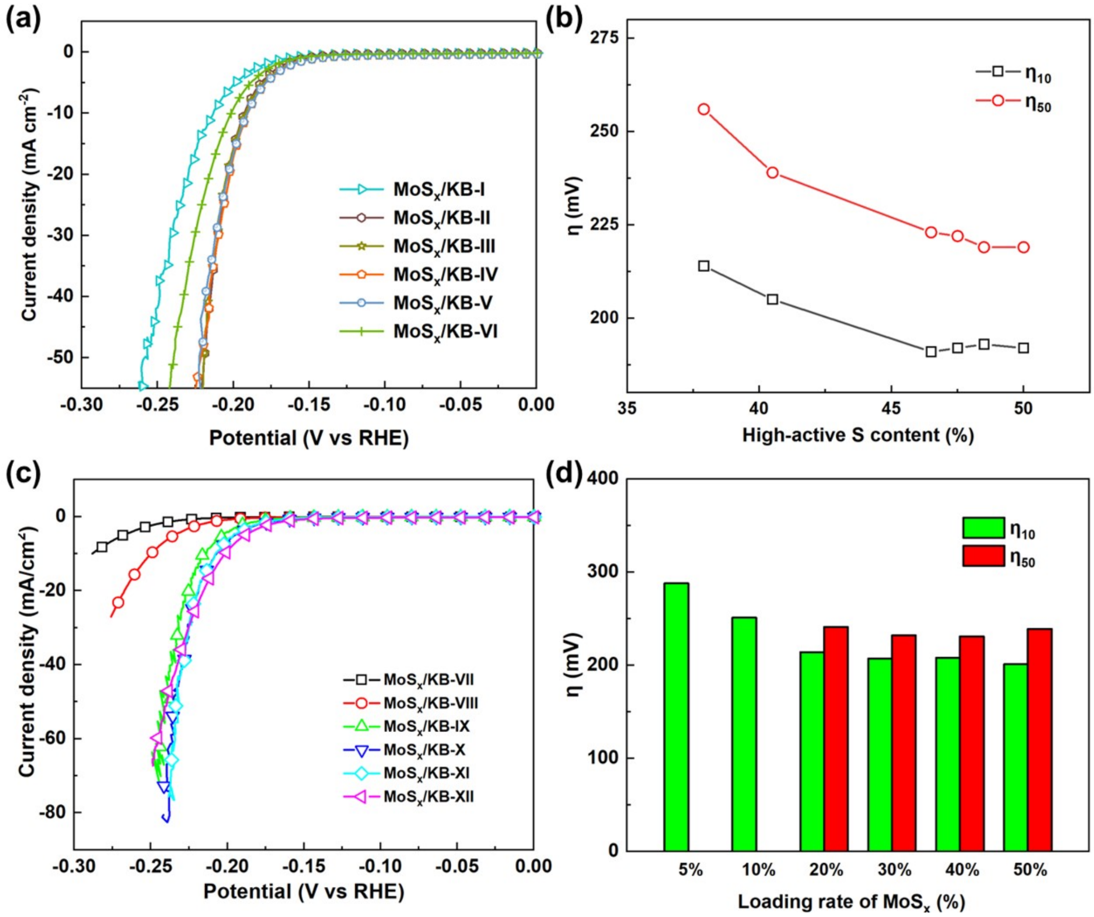

Fig. S7 (a) LSV curves of the MoS_x/KBs with different high-active S contents and (b) their corresponding η values; (c) LSV curves of the MoS_x/KBs with different MoS_x loading rates and (d) their corresponding η values.

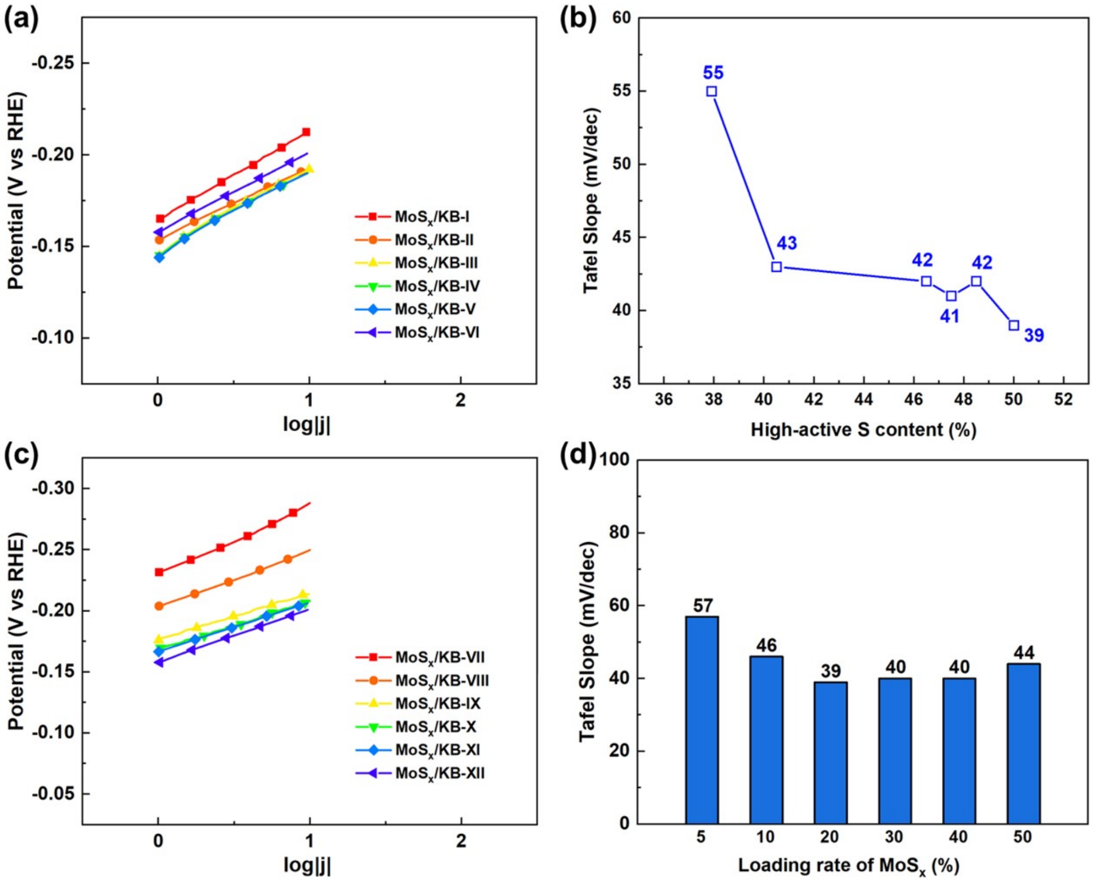

Fig. S8 (a) Tafel curves of-MoS_x/KBs with different high-active S contents and (b) their corresponding Tafel slope values; (c) Tafel curves of MoS_x/KBs with different MoS_x loading rates and (d) their corresponding Tafel slope values.

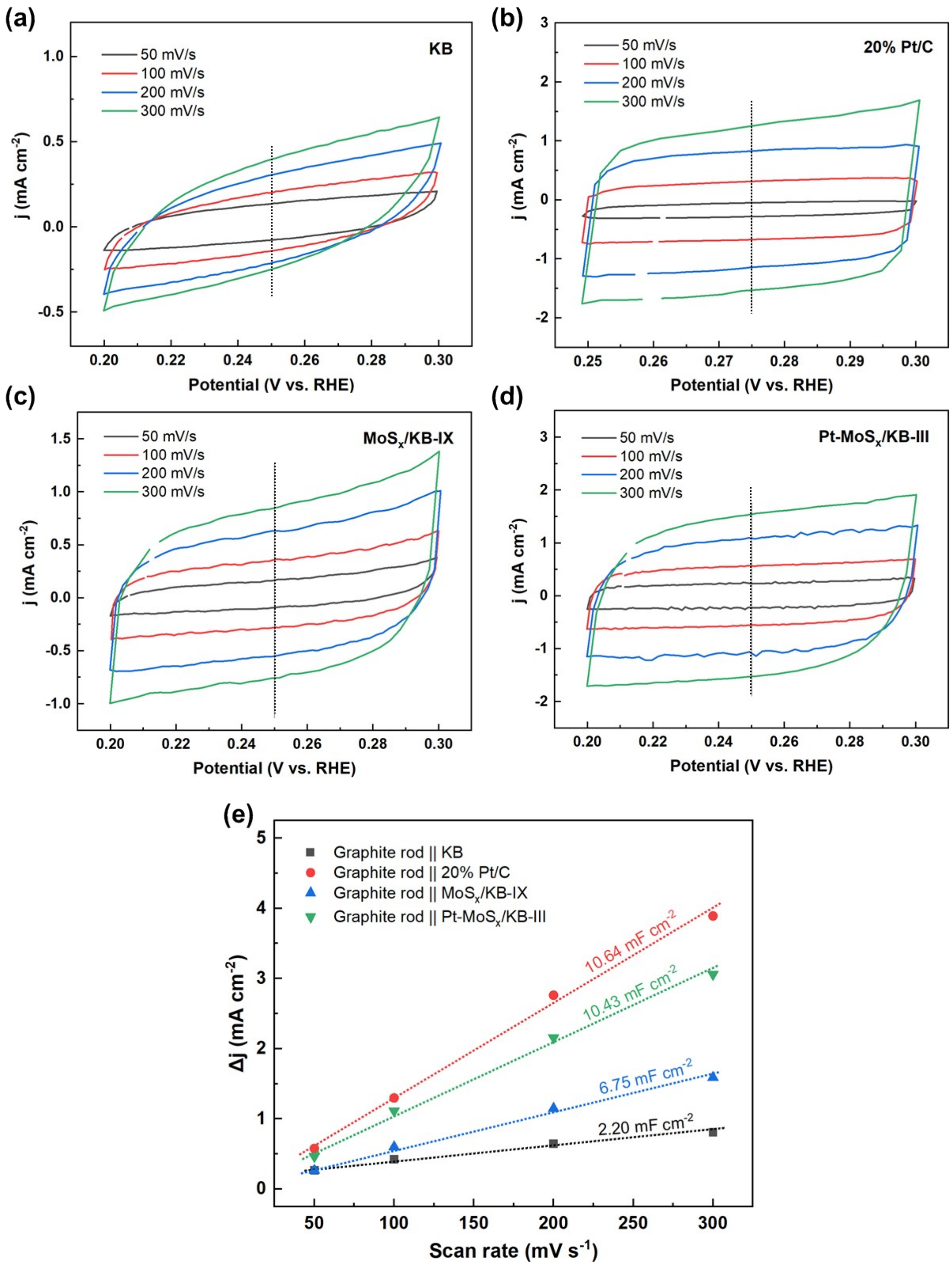

Fig. S9 CV curves of (a) KB, (b) 20% Pt/C, (c) MoS_x/KB-IX, and (d) Pt-MoS_x/KB-III catalysts measured at different scan rates. (e) Current density differences plotted against scan rates.

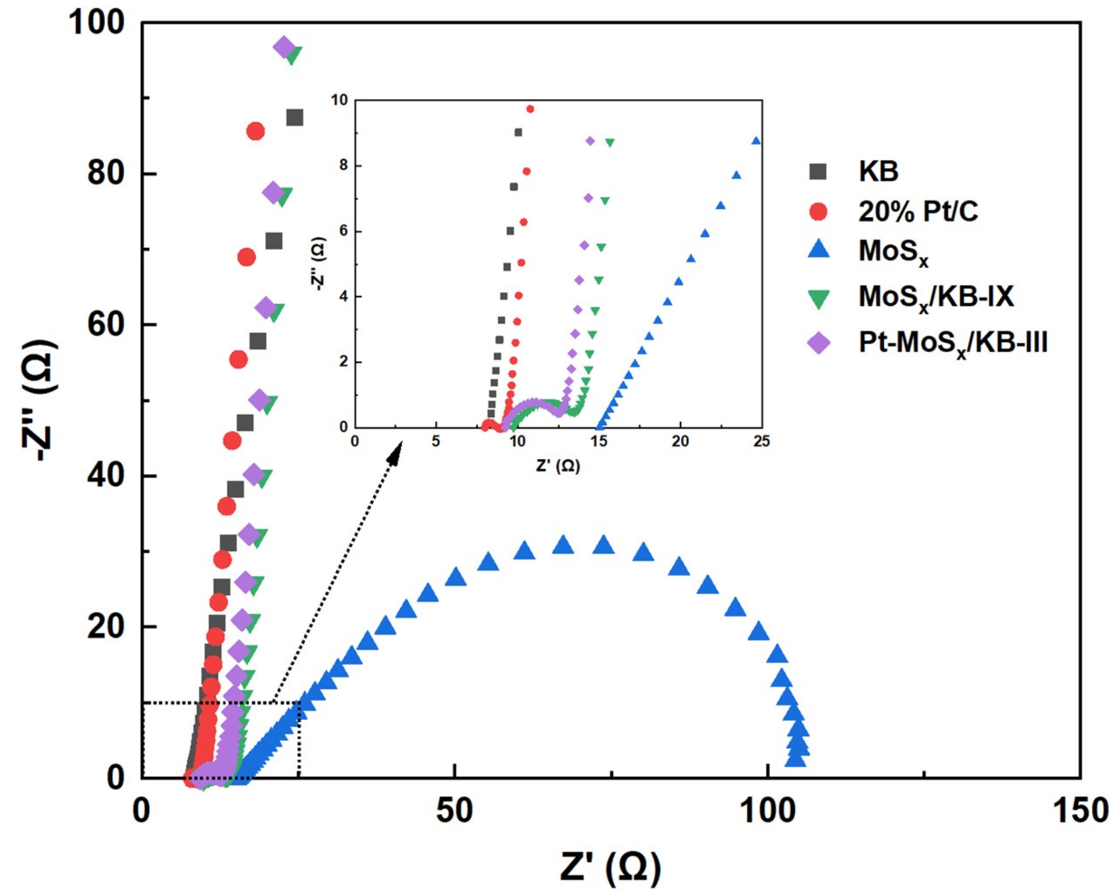

Fig. S10 Nyquist plots of KB, 20% Pt/C, MoS_x, MoS_x/KB-IX and Pt-MoS_x/KB-III.

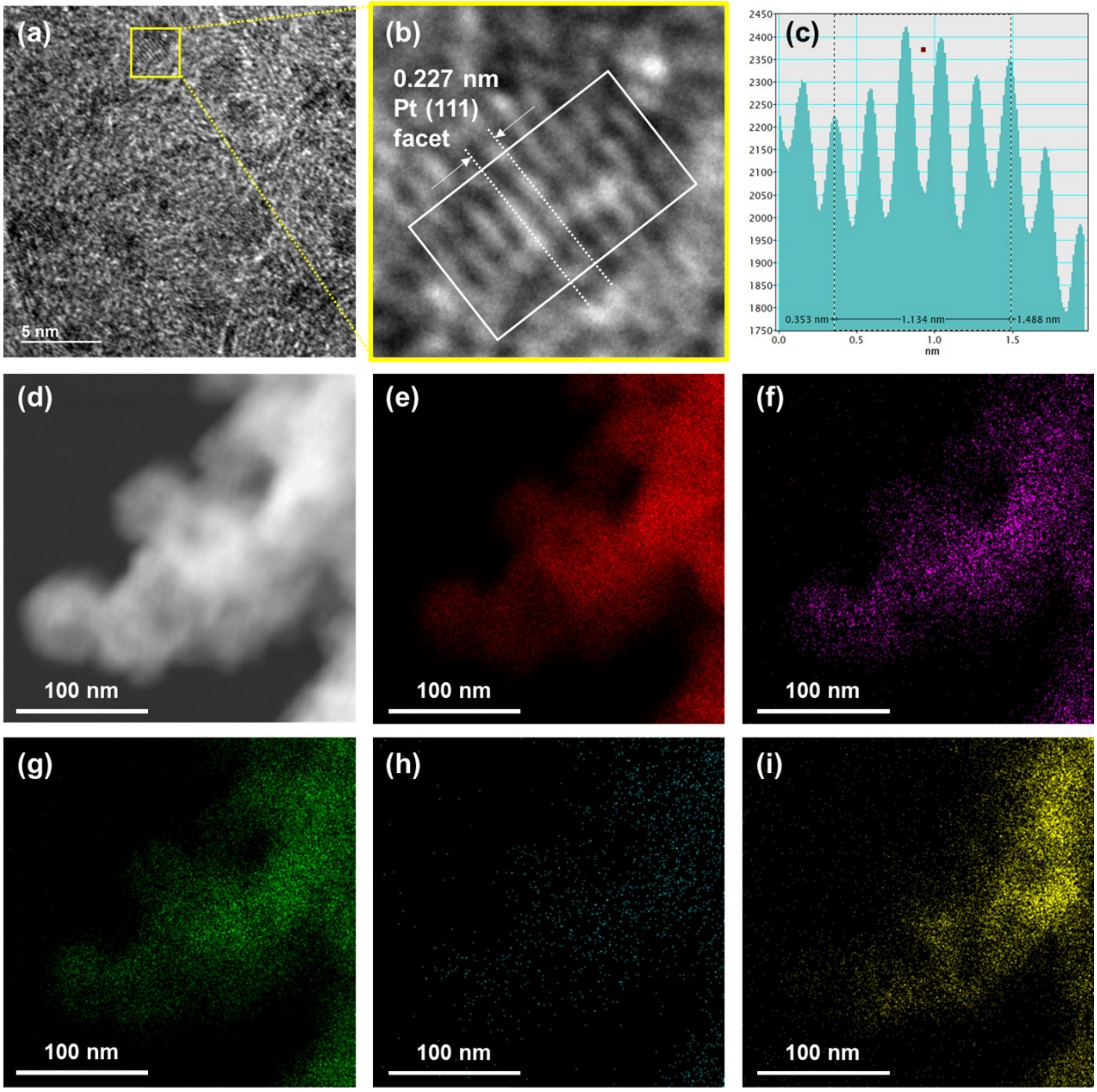

Fig. S11 (a) HR-TEM image of Pt-MoS_x/KB-III after 48h HER running at current density of 20 mA cm^{-2}. (b) The selected area for statistical crystal facet parameter of platinum and (c) the statistical result in (a). (d) STEM image and EDS mapping of (e) C, (f) Pt, (g) S, (h) Mo, and (i) F elements of Pt-MoS_x/KB-III after 48h HER running at current density of 20 mA cm^{-2}.

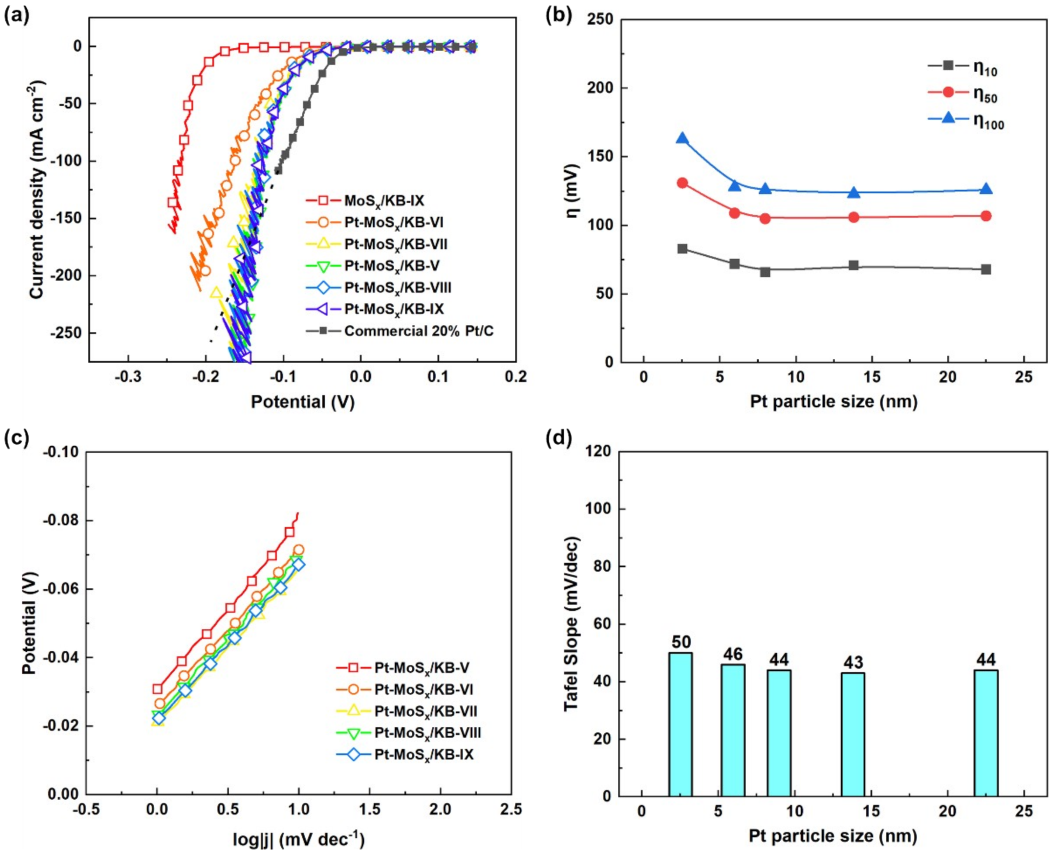

Fig. S12 (a) The LSV curve of Pt-MoS_x/KB catalysts with different Pt particle sizes, comparative MoS_x/KB-IX catalyst, and commercial 20% Pt/C catalyst in a three-electrode-system; (b) The relationship curve of the η_{10}, η_{50}, and η_{100} versus the Pt particle sizes of the Pt-MoS_x/KBs; (c) The Tafel curve of Pt-MoS_x/KB catalysts with different Pt particle sizes; (d) The Tafel slope of Pt-MoS_x/KB catalysts versus the Pt particle size.

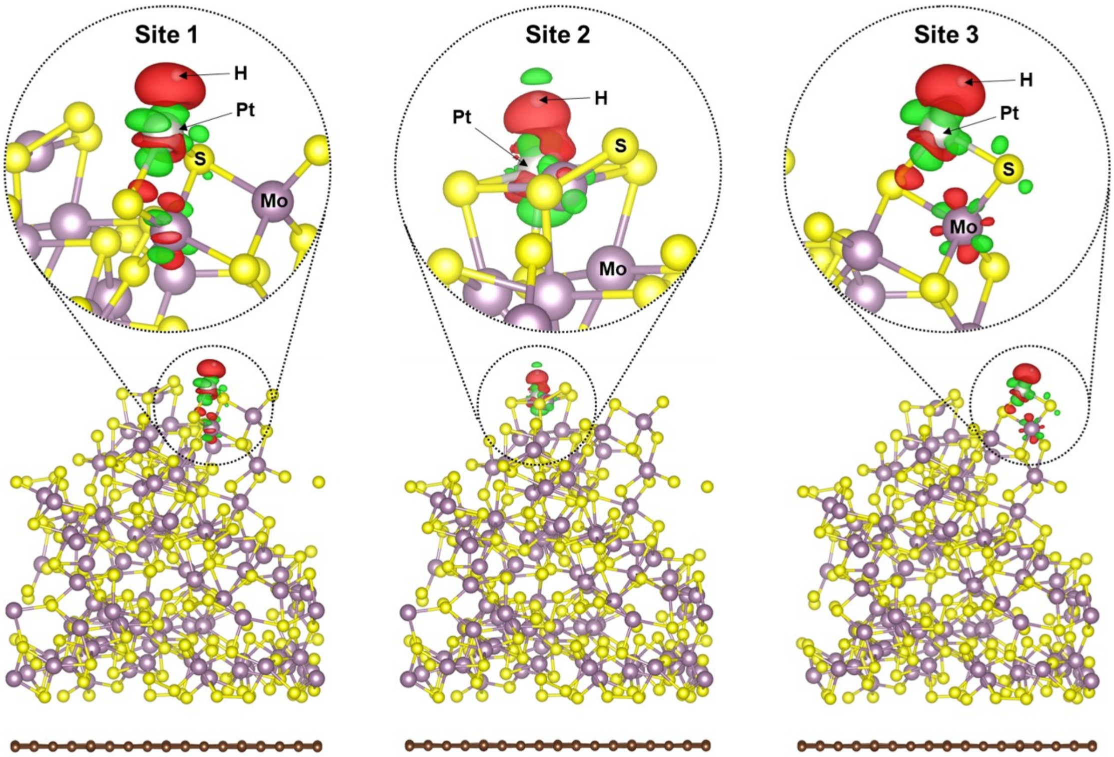

Fig. S13 Difference charge density diagram of three different sites in the Pt-MoS_x/KB model (Red: positive charge density difference, Green: negative charge density difference).

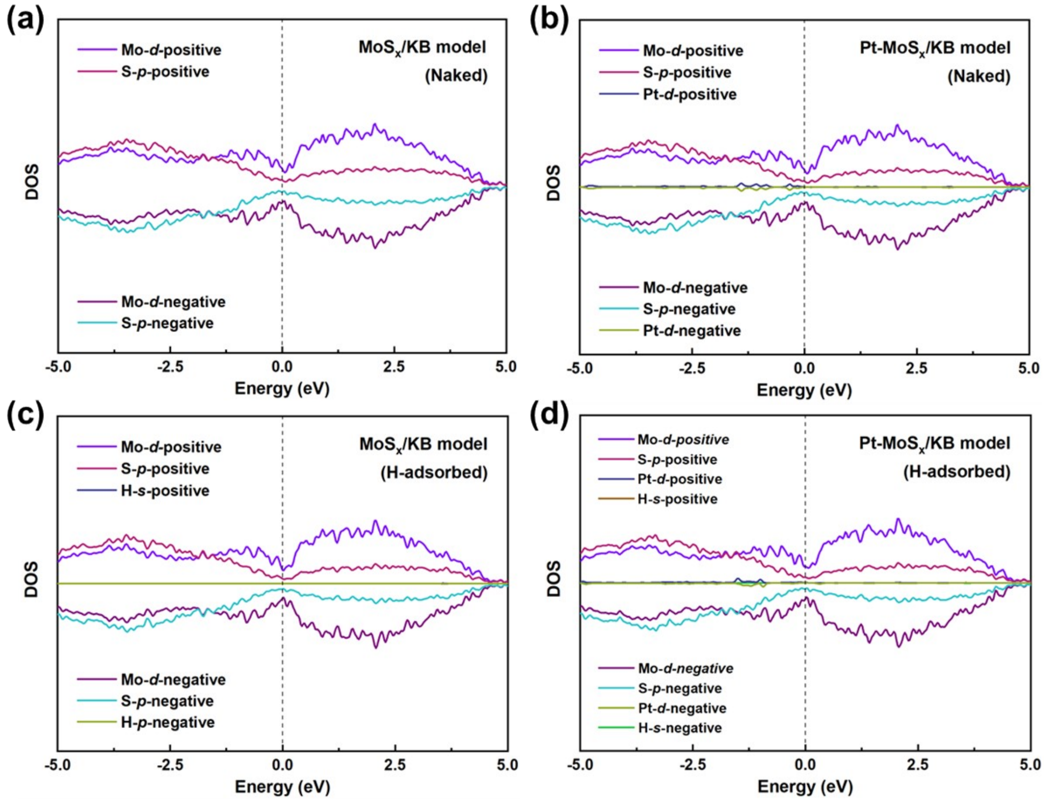

Fig. S14 The PDOS in Site 1 of (a) naked MoS_x/KB, (b) naked Pt-MoS_x/KB, (c) H-adsorbed MoS_x/KB and (d) H-adsorbed Pt-MoS_x/KB models.

Table S3 Comparison of η at different current densities and Tafel slope of Pt-MoS_x/KB-III, Pt-MoS_x/KB-IX in this work and the state-of-the-art analogous catalysts reported in recent years.

Material	Synthesis method	Pt (wt.%)	η_{10} (mV)	η_{50} (mV)	η_{100} (mV)	η_{150} (mV)	η_{200} (mV)	Tafel Slope	References
MoS_2@C supertubes	epitaxial-growth, annealing	-	93	152	180	200	220	53	[1]
$Ni_{17}W_3/WO_{3-x}/MoO_{3-x}$	Ar/H_2 reducing method	-	14	75	/	/	/	51	[2]
Ru/1T-MoS_2	hydrothermal	-	81	175	190	/	/	54	[3]
CN@CNP-Pt [a]	hydrothermal, followed by phosphitylation	1.37	22	45	75	100	120	49	[4]
Pt/CNTs-N+α-MoC_{1-x} [b]	CH_4/H_2 reducing method	2.4	17	48	78	/	/	24	[5]
NGA-COF@Pt [c]	hydrothermal	2.66	13	28	35	38	40	21.88	[6]
Pt-MoS_2	sonochemical-assisted	3	220	310	/	/	/	57	[7]
Pt-P-Ni_4Mo-Ti_4O_7/CC [d]	hydrothermal, followed by annealing	3.44	24	120	133	145	152	76	[8]
Pt/TE-UTPNBs [e]	multi-step chemical synthesis	3.71	28	55	/	/	/	31	[9]
Pt@Mo-S-Ni-CNTs [f]	annealing	5	61.2	200	/	/	/	40.2	[10]
Pt-SAs/MoS_2 [g]	site-specific electrodeposition	5.1	80	150	175	/	/	50	[11]
Pt-Ni@Re/C NPCs [h]	hydrothermal	7.3	49	80	130	200	250	29	[12]
Pt-MoS_x	electrodeposition	8.1	100	/	/	/	/	48	[13]
$PtRuP_2$ double-walled nanotubes	phosphorylation, followed by chemical etching	10	10	42	/	/	/	30.8	[14]
s-Pt/1T'-MoS_2	electrochemical intercalation, exfoliation	10	19	60	90	110	125	118	[15]
Pt-MoS_2	annealing	11	80	110	/	/	/	44	[16]

PtMo-NC [i]	pyrolysis	14.2	47	70	/	/	/	32	[17]
Pt-a-MoS_3 NDs [j]	surfactant-directed solution-phase synthesis	85	11.5	17.0	/	/	/	31.5	[18]
Pt film	calcination	100	4.2	20	27	50	75	23	[19]
Pt Nanomembrane	polymer surface buckling-enabled exfoliation	100	25	75	/	/	/	30	[20]
Commercial 20% Pt/C	-	20	34	69	103	132	162	34	-
Pt-MoS_x/KB-III	γ-ray radiation induced reduction	5.7	107	155	168	175	185	43	This work
Pt-MoS_x/KB-IX	γ-ray radiation induced reduction	13.9	66	105	126	131	149	44	This work

a. CoNi@CoNiP heterostructures implanted with ultralow loading of platinum single atoms.

b. Mechanical mixing of carbon nanotubes supported platinum nanoparticle with α-$MoC_{1-x.}$

c. Nitrogen-rich graphene analogue covalent organic frameworks supported platinum.

d. Pt and P-doped Ni_4Mo catalysts coated on one-dimensional Ti_4O_7 nanorods on carbon cloth (CC).

e. TE – terpyridine, UTPNBs – ultrathin peptoid nanobelts.

f. CNTs – carbon nanotubes.

g. SAs – single atoms.

h. NPCs – nanoparticle clusters.

i. NC – Nanocrystals.

j. Highly dispersed amorphous MoS_3 with Pt nano dendrites.

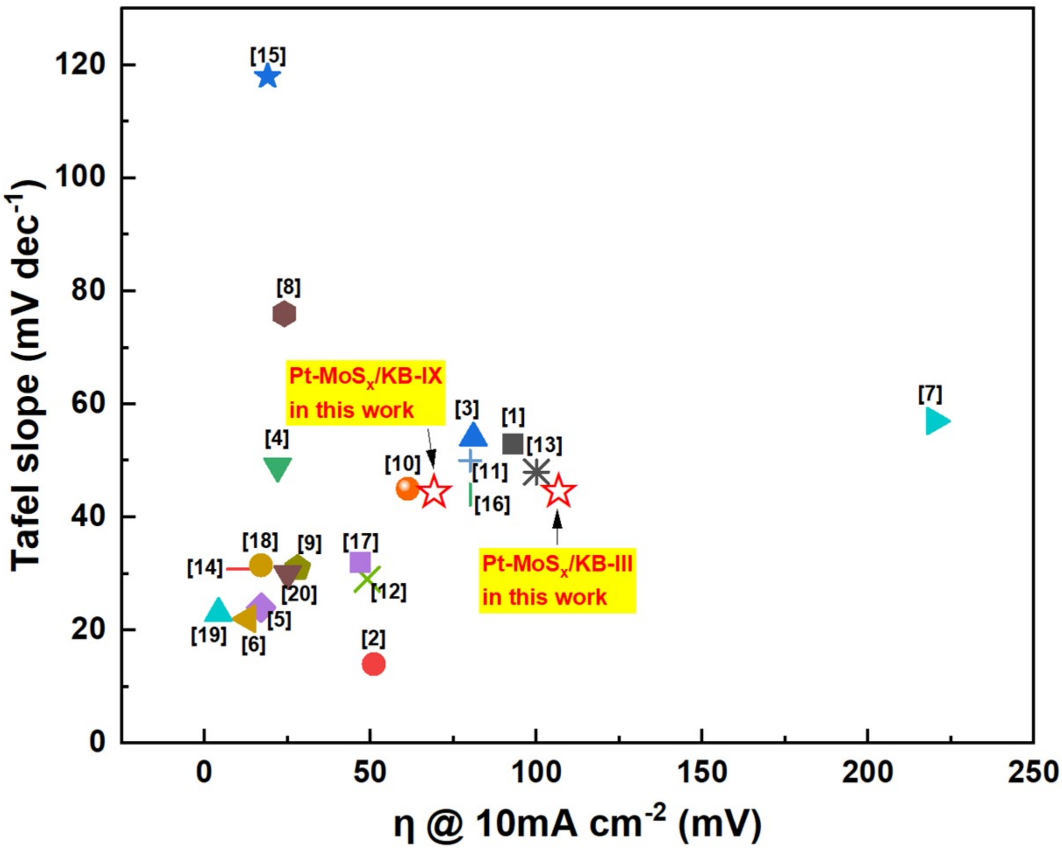

Fig. S15 The comparison of the η_{10} and the Tafel slope of the as-synthesized Pt-MoS$_x$/KB-III, Pt-MoS$_x$/KB-IX in this work and the state-of-the-art analogous catalysts reported in recent years.

References

1. W. Han, J. Ning, Y. Long, J. Qiu, W. Jiang, Y. Wang, L. Shah, D. Yang, A. Dong and T. Li, *Adv. Energy Mater.*, 2023, **13**, 2300145.
2. Y. Sun, Y. Bao, D. Yin, X. Bu, Y. Zhang, K. Yue, X. Qi, Z. Cai, Y. Li, X. Hu, J. C. Ho and X. Wang, *J. Mater. Chem. A*, 2024, DOI: 10.1039/D4TA00729H, Accepted Manuscript.
3. L. Zhu, Z. Wang, C. Li, H. Li, Y. Huang, H. Li, Z. Wu, S. Lin, N. Li, X. Zhu and Y. Sun, *J. Mater. Chem. A*, 2022, **10**, 21013-21020.
4. M. Bollu, D. T. Tran, S. Prabhakaran, D. H. Kim, N. H. Kim and J. H. Lee, *Nano Energy*, 2024, **123**, 109413.
5. H. Cai, L. Wang, W. Liu, X. Zhang, B. Chen, P. Mao, J. Fang, R. Gao and C. Shi, *Small*, 2023, **19**, 2207146.
6. Z. Zhang, Z. Zhang, C. Chen, R. Wang, M. Xie, S. Wan, R. Zhang, L. Cong, H. Lu, Y. Han, W. Xing, Z. Shi and S. Feng, *Nat. Commun.*, 2024, **15**, 2556.
7. T. H. M. Lau, S. Wu, R. Kato, T. S. Wu, J. Kulhavy, J. Y. Mo, J. W. Zheng, J. S. Foord, Y. L. Soo, K. Suenaga, M. T. Darby and S. C. E. Tsang, *ACS Catal.*, 2019, **9**, 7527-7534.
8. V. Hoa, S. Prabhakaran, M. Mai, H. T. Dao and D. Kim, *Small*, 2024, DOI: 10.1002/smll.202310666, 2310666.
9. P. Wu, P. Sui, G. Peng, Z. Sun, F. Liu, W. Yao, H. Jin and S. Lin, *Adv. Mater.*, 2024, DOI: 10.1002/adma.202312724, 2312724.
10. B. Chen, D. Wang, S. Wei and J. Wang, *Carbon*, 2024, **224**, 119061.
11. Y. Shi, W. Huang, J. Li, Y. Zhou, Z. Li, Y. Yin and X. Xia, *Nat. Commun.*, 2020, **11**, 4558.
12. J. Kim, J. Oh, S. Baskaran, T. G. Kim, S. Kim, J. Yang, J. Jung and S. M. Yoon, *Appl Catal B-Environ*, 2024, **347**, 123791.
13. X. Y. Chia, N. A. A. Sutrisnoh and M. Pumera, *ACS Appl. Mater. Interfaces*, 2018, **10**, 8702-8711.
14. Y. Hong, S. C. Cho, S. Kim, H. Jin, J. H. Seol, T. K. Lee, J. K. Ryu, G. M. Tomboc, T. Kim, H. Baik, C. Choi, J. Jo, S. Jeong, E. Lee, Y. Jung, D. Ahn, Y. T. Kim, S. J. Yoo, S. U. Lee and K. Lee, *Adv. Energy Mater.*, 2024, **14**, 2304269.
15. Z. Shi, X. Zhang, X. Lin, G. Liu, C. Ling, S. Xi, B. Chen, Y. Ge, C. Tan, Z. Lai, Z. Huang, X. Ruan, L. Zhai, L. Li, Z. Li, X. Wang, G. Nam, J. Liu, Q. He, Z. Guan, J. Wang, C. Lee, A. R. J. Kucernak and H. Zhang, *Nature*, 2023, **621**, 300-305.
16. S. Li, J. K. Lee, S. Zhou, M. Pasta and J. H. Warner, *Chem. Mater.*, 2019, **31**, 387-397.
17. H. Zhang, F. Wan, X. G. Li, X. Chen, S. Xiong and B. Xi, *Adv. Funct. Mater.*, 2023, **33**, 2306340.
18. K. Guo, J. Y. Zheng, J. C. Bao, Y. F. Li and D. D. Xu, *Small*, 2023, **19**, 2208077-2208085.
19. Z. N. Zahran, Y. Tsubonouchi, D. Chandra, T. Kanazawa, S. Nozawa, E. A. Mohamed, N. Hoshino and M. Yagi, *J. Mater. Chem. A*, 2024, **12**, 7094-7106.
20. X. Gao, S. Dai, Y. Teng, Q. Wang, Z. Zhang, Z. Yang, M. Park, H. Wang, Z. Jia, Y.

Wang and Y. Yang, *Nano-Micro Lett.*, 2024, **16**, 108.